Reactive Compatibilization of Polycarbonate and Poly(methyl methacrylate) in the Presence of a Novel Transesterification Catalyst SnCl 2 ·2H 2 O

ARTICLE *in* THE JOURNAL OF PHYSICAL CHEMISTRY B · FEBRUARY 2011

Impact Factor: 3.3 · DOI: 10.1021/jp107897a · Source: PubMed

3 AUTHORS:

Akhilesh Kumar Singh
Universidad Nacional Autónoma de México
32 PUBLICATIONS **206** CITATIONS
SEE PROFILE

Rajiv Prakash
Indian Institute of Technology (Banaras Hin…
135 PUBLICATIONS **1,351** CITATIONS
SEE PROFILE

Dhananjai Pandey
Indian Institute of Technology (Banaras Hin…
245 PUBLICATIONS **3,701** CITATIONS
SEE PROFILE

THE JOURNAL OF PHYSICAL CHEMISTRY B

ARTICLE

pubs.acs.org/JPCB

Reactive Compatibilization of Polycarbonate and Poly(methyl methacrylate) in the Presence of a Novel Transesterification Catalyst $SnCl_2 \cdot 2H_2O$

A. K. Singh, Rajiv Prakash, and Dhananjai Pandey*

School of Materials Science & Technology, Institute of Technology, Banaras Hindu University, Varanasi-221005, India

Supporting Information

ABSTRACT: We compare the effectiveness of various known organometallic transesterification catalysts with a novel $SnCl_2 \cdot 2H_2O$ transesterification catalyst in the formation of homogeneous PC/PMMA blends with single T_g. It is shown that $SnCl_2 \cdot 2H_2O$ works more efficiently than the other organometallic transesterification catalysts. Even 0.1% (wt/wt) of $SnCl_2 \cdot 2H_2O$ is enough to establish an interaction between PC and PMMA phases, leading to the formation of a homogeneous PC/PMMA blend with single T_g and single degradation temperature. FTIR, ^1H NMR, and XRD studies provide evidence of the formation of PC-*g*-PMMA graft copolymer, which acts as a compatibilizer between the PC and PMMA phases. A significant improvement in the optical transparency of the PC/10PMMA blend prepared using $SnCl_2 \cdot 2H_2O$ catalyst as compared with PC/10PMMA without any catalyst is observed. There is also a change in the morphology from granular in uncompatibilized blends to lamellar in the compatibilized blends.

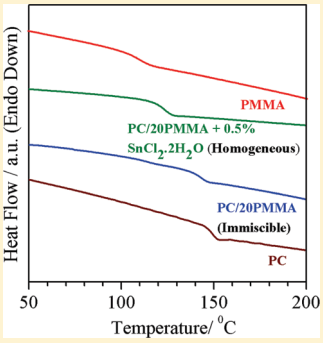

1. INTRODUCTION

Immiscible polymer blends have received enormous interest in recent years because of the possibility of combining the attractive features of each component[1,2] in the blend. However, their optimum performance, and especially the long-term stability, depends on the specific strategy adopted to compatibilize the blend components to control the size, shape, and morphology of the dispersed phase as also the interfacial adhesion to prevent coalescence of the dispersed phase. A compatibilizer acts as a surfactant, which lowers the interfacial tension between the two polymer phases and thereby promotes adhesion. The compatibilization of two polymer phases can be achieved by adding a block, graft, or cross-linked copolymer of the two polymer components in the blend or by forming such a copolymer through covalent or ionic bond formation in situ during what is commonly known as reactive compatibilization.[2] The reactive compatibilization process is generally regarded as an industrially viable technique.[2]

Among the various polymer blends, blends of bisphenol A polycarbonate (PC) with poly(methyl methacrylate) (PMMA) are one of the most studied ones.[3−39] PMMA possesses high mechanical strength and impressive optical transparency and is easy to synthesize at a low cost, but its lack of toughness severely restricts its application as an engineering plastic. PC, on the other hand, has several outstanding properties like exceptional impact resistance, dimensional stability, better ductility, and higher glass-transition temperature,[3−11] but it is much more expensive than PMMA. Blending of PC with PMMA is expected to bring down the cost without affecting the other properties significantly. Accordingly, PC/PMMA blends have been proposed for several potential applications such as gas separation membrane, pearl material, substrate of the optical data storage discs, packaging material, and so on.[12]

Although the PC/PMMA blend system has been investigated extensively, several controversies continue to abound the literature. PC/PMMA blends are generally prepared by melt mixing or solution casting techniques with or without compatibilizers. Although the PC/PMMA system is regarded as an immiscible system, the work of Butzbach and Wendorff[4] reveals weak specific interactions between the phenyl rings of PC and carbonyl group of the PMMA phase. Kim et al.[9] proposed that the compatibility in PC/PMMA blends increases on increasing the PMMA content; that is, the PMMA rich phase is more compatible than the PC rich phase. Marin et al.[17] presented evidence of cocontinuous morphology of the PC/PMMA blend. On the basis of the thermal, mechanical, and morphological studies, they suggested partial miscibility in the PC/PMMA blends. Lim and Kyu[18,31] studied the phase separation behavior of PC/PMMA blends and claimed that the blends of PC with moderately low-molecular-weight PMMA exhibit both the upper critical solution (UCST) and lower critical solution (LCST) temperatures. According to these workers, the phase separation first occurs through spinodal decomposition, but is followed by phase dissolution. Nishimoto et al.[28] showed that the phase separation above T_g of the blends is not a result of LCST but is an artifact originating

Received: August 20, 2010
Revised: December 22, 2010
Published: January 28, 2011

from the very slow rate of phase separation from the kinetically trapped metastable microstructure of PC/PMMA blends in solution cast films. Rabeony et al.,[11] suggested that the so-called phase dissolution above UCST by Lim and Kyu[18,31] is an artifact and it is actually due to the transesterification reaction between PC and PMMA phases at ∼250 °C. It is now widely recognized that the main challenge encountered in studying the phase separation behavior of PC/PMMA blends is the proximity of the T_g to the so-called LCST. To overcome this, Woo et al.[32] prepared the ternary blends of PC/PMMA and diglycidyl ether of bisphenol A (DGEBA) and studied their phase separation behavior. After annealing for a long time (150 h), they found that the phase separation in ternary blends indeed occurs at 68 °C and after that it does not show miscibility. Furthermore, upon heating the blend above 240 °C, they observed decrease in domain size (0.2 to 0.5 μm). They proposed that the blends above 240 °C, which appear transparent to visible light,[18,31] actually contain a distinct phase-separated morphology but with greatly diminished domain size less than the optical wavelength. It was thus concluded that the blends do not show miscibility above 240 °C, as claimed by the previous workers.[18,31]

In literature, several different mechanisms have been proposed for chemical reactions between PC and PMMA phases for possible compatibilization. In solution cast PC/PMMA blends, Rabeony et al.[11] suggested that ester−ester interchange reaction between PC and PMMA occurs at ∼250 °C, resulting in the in situ formation of graft copolymer that compatibilizes the two phases. Their conclusion was based on the analysis of the FTIR spectra of the acetone-soluble fraction of PC/PMMA films heated at 250 °C for different periods of time. This mechanism has been questioned by Ko et al.,[37] who proposed that the thermodegradative reaction occurring during phase separation of PC/PMMA blends leads to the grafting of PMMA macroradicals onto the PC macromolecules. They also suggested that if the chemical reaction were extensive, then the cross-linked network could be formed permanently at the interfaces, which may be useful for the improvement of interfacial adhesion. Debier et al.[38] have suggested hydrolysis of the ester bonds of the PMMA leading to the acid pendent group that may acidolyze the carbonate bonds of PC and cause cross-linking. Later on, Montaudo et al.[16] proposed that thermally activated exchange reaction cannot occur in PC/PMMA blends at ∼250 °C as claimed by Rabeony et al.[11] but requires temperatures in excess of 300 °C. Montaudo et al.,[16] however, showed that in the presence of an ester-exchange catalyst ($SnOBu_2$), the exchange reaction can take place well below 300 °C (∼230 °C), but it does not lead to the formation of PC/PMMA graft copolymer of the type suggested in ref 11. Instead, NMR evidence of an exchange reaction between the methyl methacrylate (MMA) monomer, generated in the unzipping of PMMA chains, and the carbonate groups of PC was presented.[16] Unlike the previous workers, who mostly relied on indirect methods like FTIR of acetone insoluble part, DSC, TGA, and optical transparency to infer the transesterification mechanism for copolymer formation leading to homogeneous PC/PMMA blends, Montaudo et al.[16] used direct methods like nuclear magnetic resonance (NMR), mass spectrometry (MS), and size exclusion chromatography (SEC) to support their conclusions. Besides $SnOBu_2$ used in ref 16, attempts have also been made to enhance the compatibility between PC and PMMA by using various other transesterification catalysts. For example, Penco et al.[15] used tetrabutylammonium tetraphenylborate (TBATPB) as a transesterification catalyst for PC/PMMA blend formation. They proposed FTIR and DSC evidence of ester−ester exchange reaction with the addition of 1% (wt/wt) TBATPB during melt extrusion leading to the homogeneous PC/PMMA blend formation. The ester−ester exchange reaction has also been proposed by Lee et al.[22] using titanium(IV) butoxide transesterification catalyst.

Although there are reports on the formation of homogeneous PC/PMMA blends using transesterification catalysts, these catalysts are rather expensive and are required in fairly high amount (1% wt/wt). Therefore, there is still a need for getting a cheaper and more efficient transesterification catalyst for homogeneous PC/PMMA blend formation. There is also a need for exploring the efficiency of inorganic transesterification catalysts and the associated reaction mechanisms by NMR. Taking these factors into account, we have investigated several inorganic transesterification catalysts, among which we find dihydrated stannous chloride ($SnCl_2 \cdot 2H_2O$) as a novel transesterification catalyst well suited for obtaining homogeneous PC/PMMA blends. The beauty of this transesterification catalyst is that it is very efficient, as even a trace amount of it is enough to achieve the compatibility in the PC/PMMA blends. Furthermore, it is very cheap in comparison with other transesterification catalysts based on organometallic formulations. In the present report, we give evidence of homogeneous PC/PMMA blend formation using this novel transesterification catalyst by DSC, FTIR, NMR, powder XRD, TGA, UV−vis, and AFM studies. DSC studies show single T_g in PC/PMMA blends up to 40% PMMA content prepared in the presence of 0.5% (wt/wt) transesterification catalyst $SnCl_2 \cdot 2H_2O$. TGA shows a single-step degradation of PC/PMMA blends prepared in the presence of transesterification catalyst $SnCl_2 \cdot 2H_2O$, which was not observed in the absence of the transesterification catalyst. The FTIR spectra of the acetone-insoluble portion of PC/PMMA blend suggest PC-*g*-PMMA graft copolymer formation. High-resolution ^{1}H NMR studies reveal a significant shift of the methyl ester proton's peak from 3.547 ppm in pure PMMA to 3.608 ppm in the compatibilized PC/10PMMA blend, which supports PC-*g*-PMMA graft copolymer formation. The homogeneous PC/PMMA blends obtained using this new catalyst exhibit improved transparency, a systematic shift toward lower 2θ value in the XRD peak position of PC as a function of PMMA as well as transesterification catalyst $SnCl_2 \cdot 2H_2O$ content and a homogeneous lamellar morphology.

2. EXPERIMENTAL SECTION

PMMA (IG 840, mol. weight 52 000, LG MMA), PC (Makrolon 2015 mol. weight 15 000, Bayer), $SnCl_2 \cdot 2H_2O$ (Thomas Baker, India), titanium butoxide (Himedia, India), and TBATPB (Adrich) were used for preparing PC/PMMA blends.

PC/PMMA blends in different weight ratios were prepared by melt extrusion method using a corotating twin screw extruder (Thermofisher, Hakke Mini Lab II Micro compounder). The blend components were ground and mixed thoroughly in a mixer and then extruded at an optimized temperature and screw speed of 230 °C and 50 rpm, respectively.

The glass-transition temperature of PC/PMMA blends was measured using DSC (Mettler-Toledo, 823) at a heating rate of 20 °C/min under a nitrogen atmosphere. First of all, we heat the pristine blend from 30 to 300 °C at a heating rate of 20 °C/min and then cool the sample with the maximum possible cooling rate of 45 °C/minute available with the DSC. This constitutes the first DSC run. After this, we reheat the sample from 30 to 300 °C

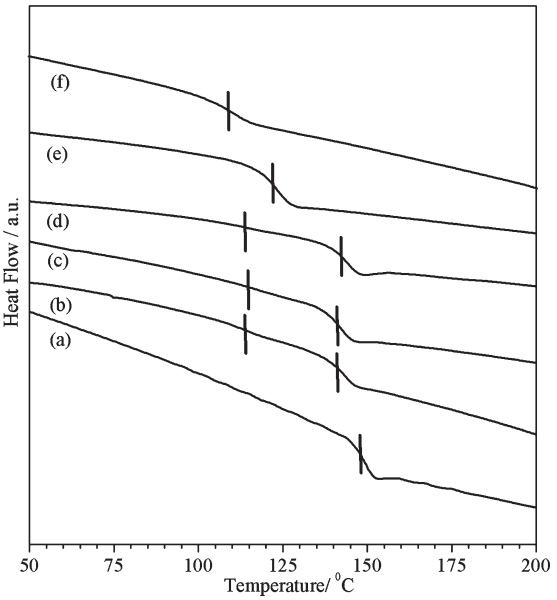

Figure 1. DSC thermograms (second run) of quenched PC/PMMA blends prepared by melt extrusion technique: (a) Pure PC, (b) PC/20PMMA blend, (c) PC/20PMMA + 0.5% tetrabutylammonium tetraphenylborate (TBATPB), (d) PC/20PMMA + 0.5% titanium butoxide, (e) PC/20PMMA +0.5% $SnCl_2 \cdot 2H_2O$, and (f) pure PMMA.

at a heating rate of 20 °C/min for recording the DSC data in the second run. The DSC was calibrated with indium and zinc before use.

The thermal degradation was studied using TGA (Mettler-Toledo, TGA/DSC-1) at a heating rate of 20 °C/min under a nitrogen atmosphere. The degradation temperature of the samples was measured on the basis of 5% weight loss.

Powder XRD patterns were recorded using an 18 KW Cu rotating-anode-based powder diffractometer fitted with curved crystal monochromator in the diffracted beam (Rigaku). The XRD data were obtained from 2θ = 5 to 60° at a scan rate of 3°/min. The X-ray generator was operated at 40 kV and 150 mA.

FTIR spectroscopic technique was used to evaluate the PC/PMMA blend formation. To achieve this, unleached and acetone-leached PC/PMMA blends were characterized using an FT-IR spectrometer (Spectrum RSi, Perkin-Elmer) with a resolution of 2 cm^{-1}.

^{1}H NMR spectra were recorded on a Bruker 500 MHz spectrometer (Avance AV 500WB) at ambient temperature in $CDCl_3$ solvent. The chemical shifts are reported in parts per million relative to tetramethylsilane.

Optical transparency of the molded PC/PMMA blend films having thickness of ~0.6 mm was measured by UV/vis spectrophotometer (Lambda 25, Perkin-Elmer).

A multimode atomic force microscope (PRO 47, NT-MDT) controlled by a scanning probe (Solver) was used for surface topographic studies of thin films of the blends in the tapping mode.

3. RESULTS AND DISCUSSION

To get more efficient and cheaper transesterification catalyst for achieving homogeneous PC/PMMA blends, we investigated several organometallic and inorganic transesterification catalysts. Figure 1 compares the effectiveness of various transesterification catalysts for the compatibility of the blend phases in the melt extruded PC/PMMA blends. For this comparative study, we concentrated on PC/20PMMA blend composition, even though our results are valid for other compositions as well. DSC thermograms of pure PC, pure PMMA, melt extruded PC/20PMMA without transesterification catalyst, and PC/20PMMA with 0.5% wt/wt of transesterification catalysts are shown in Figure 1. All of these samples were heated to 300 °C and then cooled to room temperature in a minimum possible time (~6 min) before the DSC data were recorded in the second run. PC/20PMMA without any transesterification catalyst shows two clearly distinguishable glass-transition temperatures. The lower T_g is attributable to the PMMA-rich phase, whereas the higher T_g is for the PC-rich phase. It is observed that both of the T_g values are somewhat shifted toward higher and lower temperature sides approaching each other, suggesting some interaction between PC and PMMA in the melt extruded PC/20PMMA. PC/20PMMA blends with TBATPB and titanium butoxide as transesterification catalysts also show two distinguishable glass-transition temperatures with similar shift of T_g with respect to the T_g of PC and PMMA, as in the PC/20PMMA blend obtained without any catalyst. This, suggests the insignificant effect of these transesterification catalysts on the compatibilization of the blend components in the PC/PMMA blend when used in 0.5% (wt/wt) ratio. It is reported in the literature[15,22] that 1% (wt/wt) TBATPB and titanium butoxide leads to homogeneous PC/PMMA blends with single T_g, which implies that the two T_g values shown in Figure 1 may be due to the lower transesterification catalyst content. However, in contrast, PC/20PMMA blends prepared in the presence of 0.5% (wt/wt) $SnCl_2 \cdot 2H_2O$ as transesterification catalyst show only a single glass-transition temperature. Also, the glass-transition temperature decreases drastically (by ~25 °C) with respect to the T_g of pure PC, suggesting that $SnCl_2 \cdot 2H_2O$ is working very efficiently in the formation of homogeneous PC/PMMA blends.

To optimize the content of inorganic transesterification catalyst for getting homogeneous PC/PMMA blends of varying compositions, we prepared various PC/PMMA blend compositions (PC/10PMMA, PC/20PMMA, PC/30PMMA, PC/40PMMA, and PC/50PMMA) using very small amounts of transesterification catalyst $SnCl_2 \cdot 2H_2O$ (viz. 0.1, 0.3, and 0.5% (wt/wt)). A single glass-transition temperature was observed in PC/20PMMA, PC/30PMMA, and PC/40PMMA blend compositions using 0.1, 0.3, and 0.5% concentrations of $SnCl_2 \cdot 2H_2O$, respectively (shown in Figure 2 and Figure S1 of the Supporting Information). Figure 2 shows the second DSC thermograms for different PC/PMMA blend compositions containing a fixed amount (0.5%) of $SnCl_2 \cdot 2H_2O$. It is evident from this Figure that the glass-transition temperature of PC/PMMA blends decreases systematically with increasing PMMA content up to ~50%. Two glass-transition temperatures are observed for PMMA content of 50% or more. Inset (a) to Figure 2 shows the variation of the glass-transition temperature of PC/20PMMA blend with transesterification catalyst $SnCl_2 \cdot 2H_2O$ content. The glass-transition temperature (T_g) of PC/20PMMA blend decreases drastically (by ~18 °C) as compared with pure PC. For higher $SnCl_2 \cdot 2H_2O$ contents, further decrease in T_g has been observed but at a slower rate (see inset (a) of Figure 2). Inset (b) of Figure 2 shows that the experimental value of the glass-transition temperature is ~8 °C, negatively deviated with respect to the predicted value as per linear mixture rule. This indicates pronounced interaction between PC and PMMA as a result of in

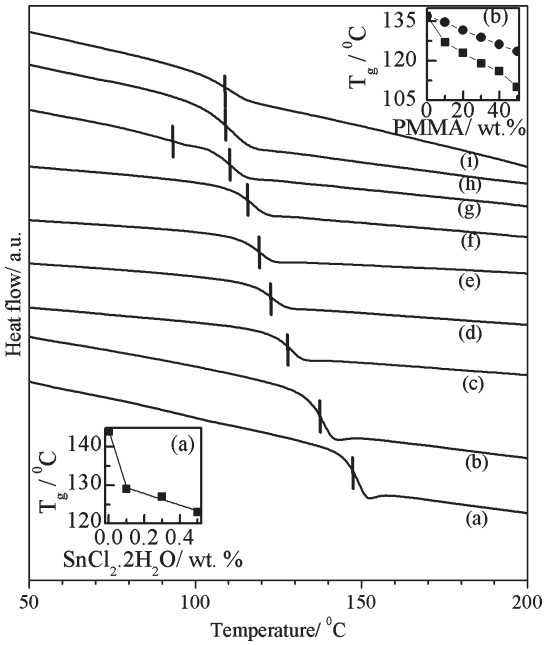

Figure 2. DSC thermograms (second run) of quenched PC/PMMA blends prepared by melt extrusion technique: (a) Extruded PC, (b) PC + 0.5% $SnCl_2 \cdot 2H_2O$, (c) PC/10PMMA + 0.5% $SnCl_2 \cdot 2H_2O$, (d) PC/20PMMA + 0.5% $SnCl_2 \cdot 2H_2O$, (e) PC/30PMMA + 0.5% $SnCl_2 \cdot 2H_2O$, (f) PC/40PMMA + 0.5% $SnCl_2 \cdot 2H_2O$, (g) PC/50PMMA + 0.5% $SnCl_2 \cdot 2H_2O$, (h) PMMA + 0.5% $SnCl_2 \cdot 2H_2O$, and (i) pure PMMA. The inset (a) shows variation of T_g with the transesterification catalyst $SnCl_2 \cdot 2H_2O$ content in PC/20PMMA blend. The inset (b) shows variation of T_g for compatibilized PC/PMMA blend (with 0.5% $SnCl_2$. $2H_2O$) with PMMA content; rectangles correspond to the experimental value of T_g, whereas the circles to T_g are predicted by linear mixture rule.

situ formation of some compatibilizer in the presence of the transesterification catalyst $SnCl_2 \cdot 2H_2O$.

To understand the mechanism of possible interchange reaction between PC and PMMA phases in the presence of $SnCl_2 \cdot 2H_2O$ as a transesterification catalyst, we carried out ^{1}H NMR studies on pure PC, pure PMMA, and the homogeneous PC/PMMA blends with single T_g. Figure 3a depicts the ^{1}H NMR spectrum of pure PC showing the characteristic proton peaks. The aromatic protons of PC are in two different environments, namely, ortho and meta with respect to the $-O-\overset{O}{\overset{\|}{C}}-O-$ group shown as 1 and 1′ in Scheme 1 given below. The ortho protons give rise to a doublet at 7.248 ppm, whereas meta gives another doublet at 7.180 ppm. In addition, the methyl group proton of bisphenol A gives a singlet at 1.685 ppm. The inset of Figure 3a shows the zoomed profile in the range of 7.1 to 7.3 ppm to reveal the multiplets. The two small peaks at 1.328 and 1.553 in this spectrum are due to the solvent. In pure PMMA, there are three different proton environments corresponding to methyl ester ($-OCH_3-$), methyl ($-CH_3$), and methyl ($-CH_2-$) shown as 3, 4, 5 in Scheme 1. These three different proton environments give rise to ^{1}H NMR peaks at 3.547 (singlet), 0.791 (multiplet), and 1.761 (multiplet) ppm, as shown in Figure 3b. In the presence of catalyst, the PC chain is reported to break at $(-O-\overset{O}{\overset{\|}{C}}-O-)$ site.[16] The two broken components are reported to link with methyl ester group ($-OCH_3$) of PMMA and the remaining part of the PMMA chain, as shown in Scheme 1.[16] If such

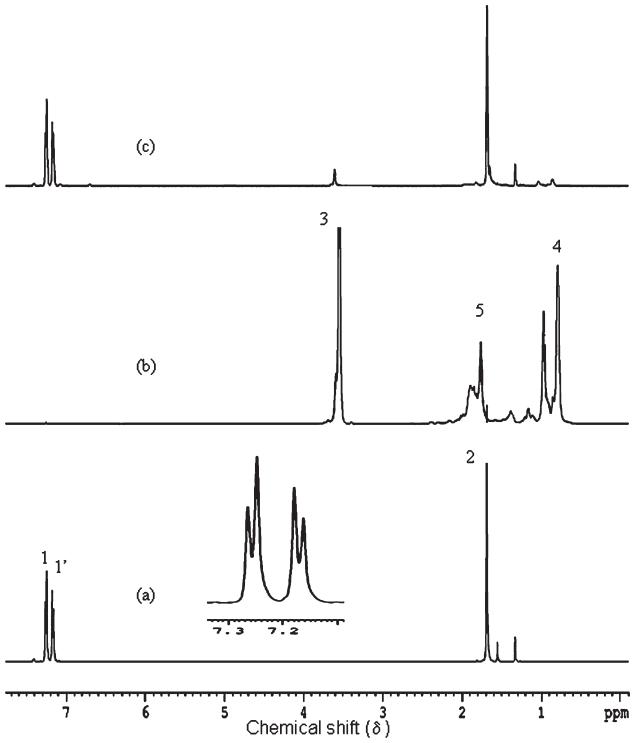

Figure 3. ^{1}H NMR spectrum of (a) PC, (b) PMMA, and (c) PC/10PMMA + 0.3% $SnCl_2 \cdot 2H_2O$ transesterification catalyst. Inset of Figure 3a shows the zoomed NMR spectrum of PC in the range of 7.1 to 7.3 ppm.

a grafting of PC and PMMA takes place, then the environment of methyl ester protons would change with respect to that in pure PMMA chain. This change of environment is indeed manifested in the ^{1}H NMR spectrum of PC/10PMMA blend prepared in the presence of 0.5% $SnCl_2 \cdot 2H_2O$ shown in Figure 3c as a shift of the methyl ester proton's peak from 3.547 ppm in pure PMMA to 3.608 ppm in the PC/10PMMA blend. Our mechanism for the formation of PC/PMMA copolymer, which acts as a compatibilizer, differs from that proposed by Montaudo et al.[16] These workers used $SnOBu_2$ as a catalyst and found evidence of new ^{1}H NMR peaks at 3.8, 5.5, and 6.1 ppm due to depolymerization of PMMA. It is evident from Figure 3c that no such peaks are present in the NMR spectrum of our blend. We therefore propose that the grafting of PC with PMMA in the presence of the transesterification catalyst $SnCl_2 \cdot 2H_2O$ takes place by the cleavage of the bonds in the vicinity of $(-O-\overset{O}{\overset{\|}{C}}-O-)$ of PC chain and its linkage with the methyl ester group of PMMA chain. We believe that this grafted macromolecule acts as a compatibilizer giving rise to homogeneous PC/PMMA blends

To check the validity of the above mechanism of PC-*g*-PMMA graft copolymer formation, we followed the method of preferential leaching out of PMMA from the PC/PMMA blends.[11,15,19] Acetone was chosen as a solvent because it acts as a good solvent for PMMA and nonsolvent for PC. PC/20PMMA blend composition was selected as the representative composition to study the effect of transesterification catalyst $SnCl_2 \cdot 2H_2O$ on graft copolymer formation. PC/20PMMA blends prepared with and without 0.3% (wt/wt) $SnCl_2 \cdot 2H_2O$ were dipped in sufficient quantity of acetone (~1% dilution) for 2 days. After that, the excess acetone was removed, and the same process was repeated thrice. Figure 4 depicts the FTIR spectra of pure PC, PC/20PMMA,

Scheme 1. Mechanism of PC-*g*-PMMA Graft Copolymer Formation

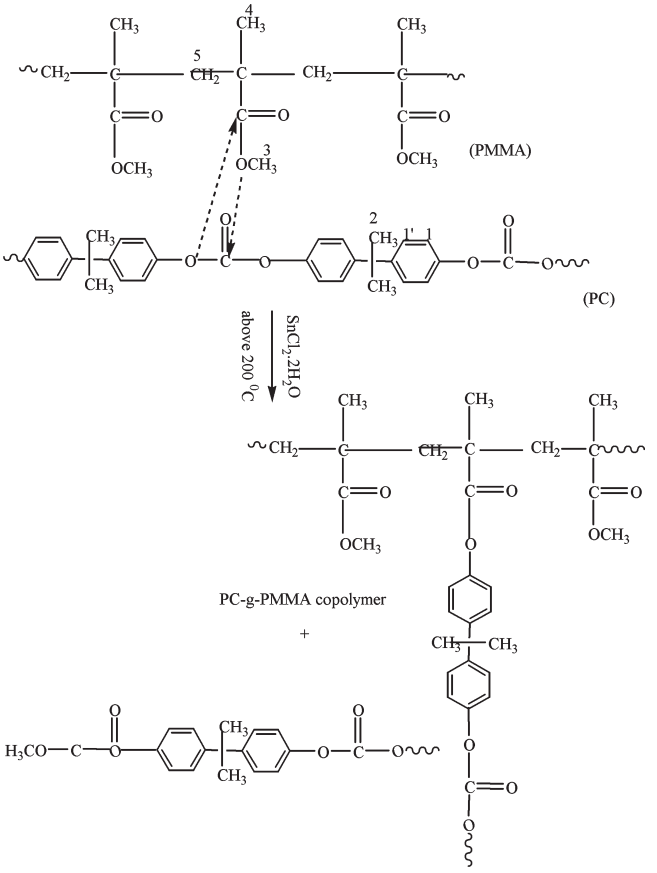

acetone-insoluble portion of PC/20PMMA, PC/20PMMA + 0.3% $SnCl_2 \cdot 2H_2O$, acetone-insoluble portion of PC/20PMMA + 0.3% $SnCl_2 \cdot 2H_2O$, and pure PMMA. The FTIR spectra of the PC/20PMMA blends in Figure 4b show two clear distinguishable carbonyl stretching vibration peaks at 1773 and 1733 cm^{-1} corresponding to the carbonyl group of PC and PMMA, respectively, whereas the same sample after acetone leaching shows the carbonyl peak of PC only, as can be seen from Figure 4c. The acetone-insoluble portion of PC/20PMMA containing 0.3% $SnCl_2 \cdot 2H_2O$ continues to show the carbonyl vibrational peaks of PC and PMMA both (Figure 4e), similar to the pristine PC/20PMMA + 0.3% $SnCl_2 \cdot 2H_2O$ (wt/wt) blend (Figure 4d). This is illustrated by deconvoluting the profiles of the two overlapping carbonyl peaks in the FTIR spectra shown in a separate panel of Figure 4. A significant decrease in the intensity of the PMMA carbonyl peak in the leached sample with respect to the unleached sample for the prepared blends in the presence of catalyst suggests the presence of some uncompatibilized PMMA homopolymer, which got leached out after acetone treatment. Furthermore, we also observe a change in the intensity of the peak due to the symmetric deformation of the $C-CH_3$ group at 870 cm^{-1}. These results further corroborate the conclusions arrived at on the basis of ^1H NMR spectra about the PC-*g*-PMMA formation in the presence of $SnCl_2 \cdot 2H_2O$ catalyst.

Figure 5 shows the TGA thermograms of PC beads, extruded PC, extruded PC/20PMMA, extruded PC/20PMMA + 0.3% transesterification catalyst $SnCl_2 \cdot 2H_2O$, and PMMA beads. We have determined the degradation temperature at 5% degradation

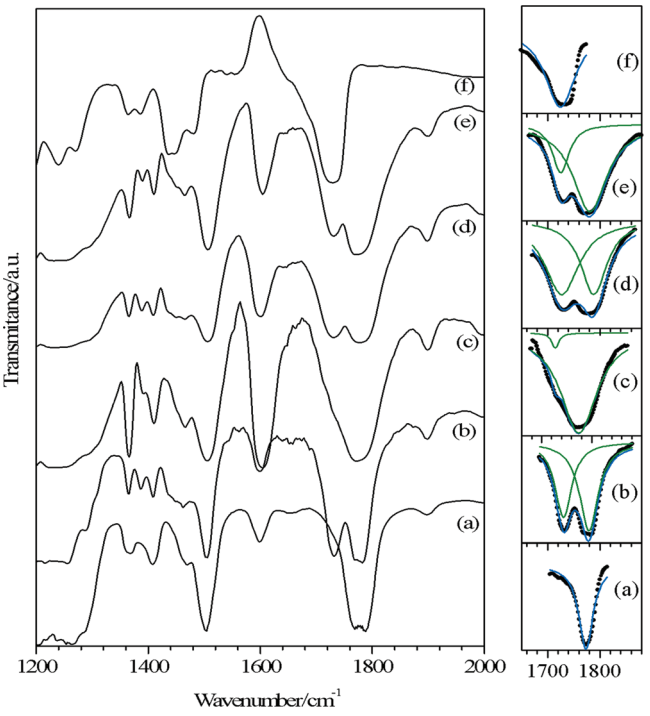

Figure 4. FTIR spectra of: (a) pure PC, (b) PC/20PMMA, (c) acetone insoluble portion of PC/20PMMA, (d) PC/20PMMA + 0.3% $SnCl_2 \cdot 2H_2O$, (e) acetone insoluble portion of PC/20PMMA + 0.3% $SnCl_2 \cdot 2H_2O$, and (f) pure PMMA prepared by melt extrusion method. In the right side, we have given the deconvoluted profile of the carbonyl peaks.

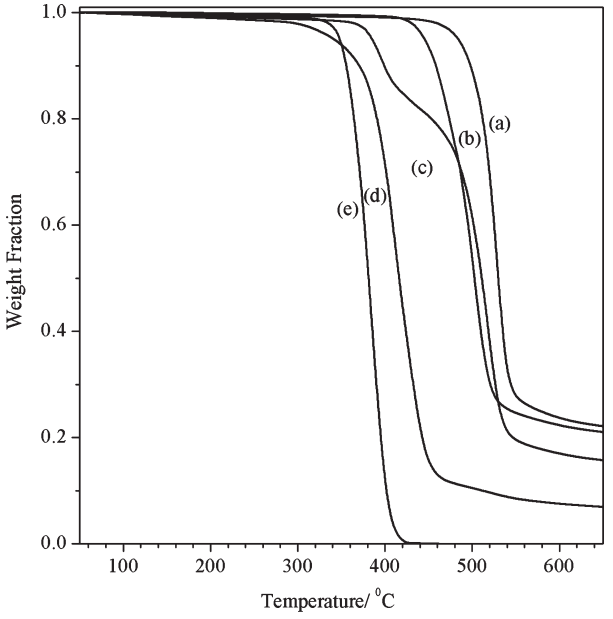

Figure 5. TGA of (a) PC bead, (b) extruded PC, (c) PC/20PMMA blend, (d) PC/20PMMA blend with 0.3% $SnCl_2 \cdot 2H_2O$, and (e) pure PMMA.

and found these to be 483, 445, 384, 340, and 347 °C for PC beads, extruded PC, extruded PC/20PMMA, extruded PC/20PMMA + 0.3% transesterification catalyst $SnCl_2 \cdot 2H_2O$, and PMMA beads, respectively. Therefore, the TGA thermograms

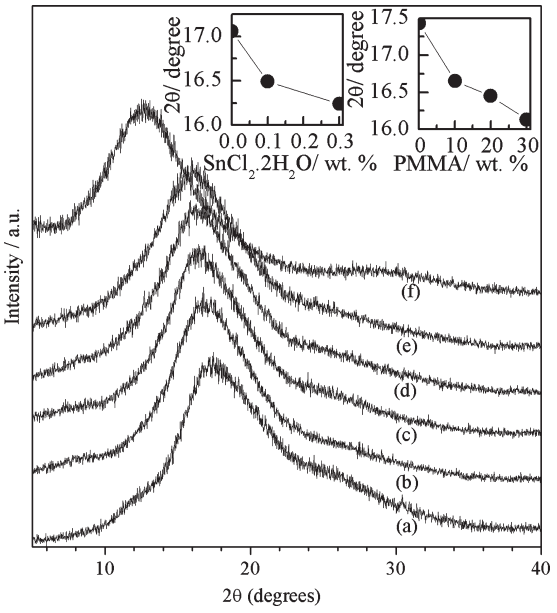

Figure 6. Powder XRD pattern of: (a) pure PC, (b) PC/10PMMA, (c) PC/10PMMA + 0.3% $SnCl_2 \cdot 2H_2O$, (d) PC/20PMMA + 0.3% $SnCl_2 \cdot 2H_2O$, (e) PC/30PMMA+ 0.3% $SnCl_2 \cdot 2H_2O$, and (f) pure PMMA prepared by melt extrusion method. Insets show the variation of the position of the characteristic PC peak as a function of transesterification catalyst content for PC/20PMMA blend composition and the PMMA content.

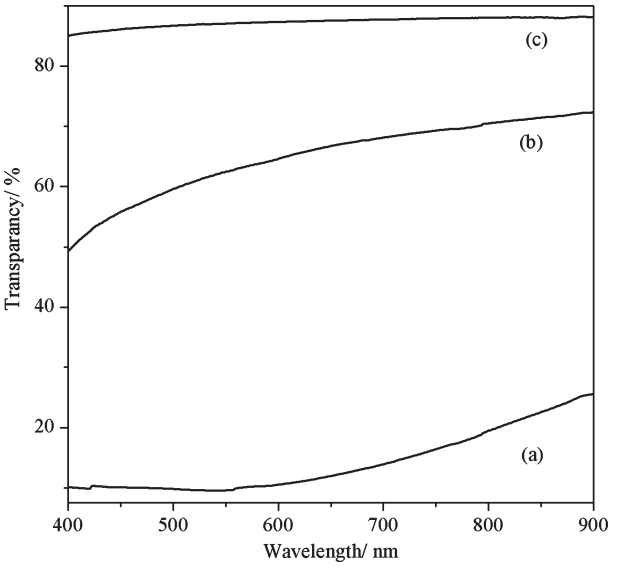

Figure 7. Optical transparency of: (a) PC/10PMMA, (b) PC/10PMMA + 0.3% $SnCl_2 \cdot 2H_2O$, and (c) pure PC having film thickness of 0.6 mm.

show a ~35 °C decrease in the degradation temperature of extruded PC as compared with that of the PC beads. This may be due to the conformational changes occurring during the extrusion process, which lead to the degradation of the material at a lower temperature. The PC/20PMMA blend without any transesterification catalyst shows two separate thermal degradation steps corresponding to PC and PMMA, suggesting insignificant interaction between the two phases. In contrast, we observe single-step thermal degradation of PC/20PMMA containing 0.3% $SnCl_2 \cdot 2H_2O$, suggesting the formation of a homogeneous blend of the two phases in the presence of transesterification catalyst. There is a slight decrease in degradation temperature (by ~40 °C) of PC/20PMMA blends containing transesterification catalyst with respect to the PC/20PMMA blends without the catalyst, which may be due to degradation caused by the catalyst.[16] Rincón and McNeill[39] have proposed a mechanism for the degradation behavior of PC/PMMA blends in the absence of any catalyst. They showed that in PC/PMMA blends the decomposition rate of PC is increased, whereas the break down of PMMA occurs at slightly higher temperatures. They proposed that during the degradation of PC/PMMA blends, interaction between degrading PMMA radicals and the PC molecules takes place, which leads to the formation of PC macroradicals with their active centers within the chain length, providing sites in the vicinity of which chain scission is likely to occur in PC. This lowers the degradation temperature of PC in PC/PMMA blends.

The XRD patterns of the melt extruded PC, PMMA, and PC/PMMA blends with 0.3% (wt/wt) transesterification catalyst are shown in Figure 6. All XRD patterns reveal the amorphous nature of pure phases as well as the blends due to the quenching effect. For pure PC, we observe a single diffuse XRD peak centered at $2\theta \approx 17.7°$, which is known to be due to the interference between the chains.[33−34] Similarly pure PMMA also shows a single broad peak centered at $2\theta \approx 12.7°$. In the PC/PMMA blends formed in the presence of transesterification catalyst, the characteristic XRD peak of PC (at $2\theta \approx 17.7°$) shifts slightly toward the lower 2θ side. The two insets to Figure 6 show the variation of the position of the characteristic peak of PC with PMMA and transesterification catalyst contents. It is evident from the insets that as the PMMA content increases for a fixed transesterification catalyst content (0.3%), the PC peak shifts toward lower 2θ angle, which signifies that interchain spacing is increasing with increasing PMMA content. Furthermore, for a fixed blend composition (PC/20PMMA) also, the PC peak shifts toward the lower 2θ side with increasing transesterification catalyst content. These observations support graft copolymer formation, which is expected to increase the interchain spacing.

Figure 7 shows the optical transparency of pure PC, PC/10PMMA, and PC/10PMMA with 0.3% (wt/wt) transesterification catalyst $SnCl_2 \cdot 2H_2O$ measured by UV/vis spectrophotometer. The films were prepared by a commercial molding machine used for the DVD dummy substrate preparation having thickness of 0.6 mm. The optical transparency of PC was found to be ~85% in the 400−900 nm region, whereas for PC/10PMMA blends without transesterification catalyst, the optical transparency is found to be ~20% only for 900 nm wavelength, and it decreases further for lower wavelengths. For PC/10PMMA with 0.3% (wt/wt) transesterification catalyst $SnCl_2 \cdot 2H_2O$, we observe ~65% optical transparency at 900 nm wavelength, which of course decreases for the lower wavelengths. Therefore, it is observed that by adding 0.3% (wt/wt) transesterification catalyst $SnCl_2 \cdot 2H_2O$ to the PC/PMMA blend, optical transparency improves significantly. This may be attributed to the absence of scattering from PC and PMMA interfaces as a result of graft copolymer formation.

Figure 8 shows the AFM images of PC/20PMMA blends without and with 0.3% transesterification catalyst $SnCl_2 \cdot 2H_2O$. Granular morphology is observed in PC/20PMMA blends without the catalyst, whereas homogeneous lamellar morphology is observed for PC/20PMMA blends containing the transesterification catalyst. This observation further supports our DSC,

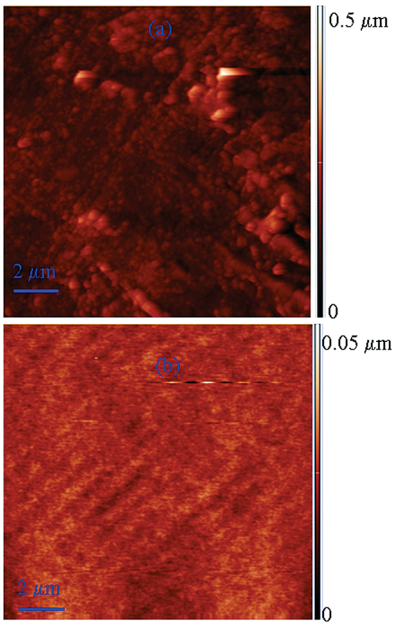

Figure 8. AFM image of (a) PC/20PMMA and (b) PC/20PMMA + 0.3% $SnCl_2 \cdot 2H_2O$ blend.

^{1}H NMR, FTIR, and TGA findings about the formation of homogeneous PC/PMMA blends in the presence of transesterification catalyst $SnCl_2 \cdot 2H_2O$.

4. CONCLUSIONS

A comparative DSC study of PC/PMMA blends prepared in the presence of various transesterification catalysts reveals that $SnCl_2 \cdot 2H_2O$ works more efficiently than the organometallic transesterification catalysts known until date. Our results show that even 0.1% (wt/wt) $SnCl_2 \cdot 2H_2O$ is enough to establish an interaction between PC and PMMA phases so as to lead to homogeneous PC/PMMA blend formation with single T_g. FTIR, ^{1}H NMR, and XRD analysis provide evidence of PC-*g*-PMMA graft copolymer formation, which acts as a compatibilizer for the two blend components. These blends show significantly higher transparency as compared with the uncompatibilized blends and homogeneous lamellar morphology.

■ ASSOCIATED CONTENT

Supporting Information. DSC thermograms of PC/PMMA blend with 0.1 and 0.3% (wt/wt) $SnCl_2 \cdot 2H_2O$ prepared using reactive extrusion technique. This material is available free of charge via the Internet at http://pubs.acs.org.

■ AUTHOR INFORMATION

Corresponding Author

*E-mail: dpandey_bhu@yahoo.co.in.

■ ACKNOWLEDGMENT

Financial support from Department of Information Technology and Moser Baer India Limited (MBIL), India is gratefully acknowledged. Mr. A. K. Singh acknowledges CSIR, India for the award of a Senior Research Fellowship. We thank Prof. B. M. Mandal for several helpful discussions and for reading the manuscript. We also thank Dr. Pralay Maiti, Dr. Nira Misra, Dr. B. Ray, and Dr. Akhilesh Kumar Singh for helpful discussions.

■ REFERENCES

(1) Paul, D. R.; Bucknall, C. B. *Polymer Blends*; John & Sons. Inc: New York, 2000.
(2) Utracki, L. A. *Polymer Blends Handbook*; Kluwer Academic Publisher: Dordrecht, The Netherlands, 1999.
(3) Agari, Y.; Ueda, A.; Omura, Y.; Nagai, S. *Polymer* **1997**, *38*, 801.
(4) Butzbach, G. D.; Wendorff, J. H. *Polymer* **1991**, *32*, 1155.
(5) Chiou, J. S.; Barlow, J. W.; Paul, D. R. *J. Polym. Sci., Part B: Polym. Phys.* **1987**, *25*, 1459.
(6) Saldanha, J. M.; Kyu, T. *Macromolecules* **1987**, *20*, 2840.
(7) Kyu, T.; Saldanha, J. M. *Macromolecules* **1988**, *21*, 1021.
(8) Sakellariou, P.; Eastmond, G. C. *Polymer* **1993**, *34*, 1528.
(9) Kim, W. N.; Burns, C. M. *Macromolecules* **1987**, *20*, 1876.
(10) Woo, E. M.; Su, C. C. *Polymer* **1996**, *37*, 5186.
(11) Rabeony, M.; Heeih, D. T.; Garner, R. T.; Peiffer, D. G. *J. Chem. Phys.* **1992**, *97*, 4505.
(12) An, N.; Yang, Y.; Dong, L. *Macromolecules* **2007**, *40*, 306.
(13) Ray, S. R.; Bousmina, M. *Macromol. Rapid Commun.* **2005**, *26*, 1639.
(14) Ray, S. R.; Bousmina, M.; Maazouz, A. *Polym. Eng. Sci.* **2006**, 1121.
(15) Penco, M.; Sartore, L.; Sciucca, S. D.; Landro, L. D.; D'Amore, A. *Macromol. Symp.* **2007**, *247*, 252.
(16) Montaudo, G.; Puglisi, C.; Damperi, F. *J. Polym. Sci., Part A: Polym. Chem.* **1998**, *36*, 1873.
(17) Marin, N.; Favis, B. D. *Polymer* **2002**, *43*, 4723.
(18) Lim, D. S.; Kyu, T. *J. Chem. Phys.* **1990**, *92*, 3944.
(19) Choi, M.; Lee, K.; Lee, J.; Kim, H. *Macromol. Symp.* **2007**, *249*, 350.
(20) Okamoto, M. *J. Appl. Polym. Sci.* **2001**, *80*, 2670.
(21) Okamoto, M. *J. Appl. Polym. Sci.* **2002**, *83*, 2774.
(22) Lee, M. S.; Ha, M. K.; Lee, H. S.; Jo, W. H. *J. Korean Fiber Soc.* **2001**, *38*, 101.
(23) Kyu, T.; Saldanha, J. M. *J. Polym. Sci., Polym. Lett.* **1988**, *26*, 33.
(24) Kyu, T.; Saldanha, J. M. U.S. Patent 47,743,654, 1988.
(25) Kyu, T. U.S. Patent 5,049,619, 1991.
(26) Olabisi, O.; Robeson, L. M.; Shaw, M. T. *Polymer−Polymer Miscibility*; Academic Press: New York, 1979.
(27) Viville, P.; Biscarini, F.; Breadas, J. L.; Lazzaroni, R. *J. Phys. Chem. B* **2001**, *105*, 7499.
(28) Nishimoto, M.; Keshkkula, H.; Paul, D. R. *Polymer* **1991**, *32*, 272.
(29) Woo, E. M.; Su, C. C. *Polymer* **1996**, *37*, 4111.
(30) Hsu, W. P. *J. Appl. Polym. Sci.* **2001**, *80*, 2842.
(31) Kyu, T.; Lim, D. S. *J. Phys. Chem. B* **1990**, *92*, 3951.
(32) Woo, E. M.; Wu, M. N. *Polymer* **1996**, *37*, 1907.
(33) Mitchell, G. R.; Windle, A. H. *Colloid Polym. Sci.* **1985**, *263*, 280.
(34) Windle, A. H. *Pure Appl. Chem.* **1985**, *57*, 1627.
(35) Singh, A. K.; Mishra, R. K.; Prakash, R.; Maiti, P.; Singh, A. K; Pandey, D. *Chem. Phys. Lett.* **2010**, *486*, 32.
(36) Velasco, D. S.; de Moura, A. P.; Medina, A. N.; Baesso, M. L.; Rubira, A. F.; Cremona, M.; Bento, A. C. *J. Phys. Chem. B* **2010**, *114*, 5657.
(37) Ko, C. C.; Kyu, T.; Smith, S. D. *J. Polym. Sci., Part B: Polym. Phys.* **1995**, *33*, 517.
(38) Debier, D.; Devaux, J.; Legras, R *J. Polym. Sci, Part A: Polym. Chem.* **1995**, *33*, 407.
(39) Rincón, A; McNeill, I. C. *Polym. Degrad. Stab.* **1987**, *18*, 99.